



# Efficient Computation of the Radiated Sound Power of Vibrating Structures using a Modal Approach

N. Roy<sup>a</sup> and M. Lapi<sup>b</sup>

<sup>a</sup>Top Modal, 5, rue de la ZA de Ribaute, 31130 Quint-Fonsegrives, France

<sup>b</sup>DGA/DCE/CTSN, Site du Mourillon, BP 28, 83800 Toulon Armées, France

nicolas.roy@topmodal.fr

The optimal design of structures in terms of noise control is of great interest in many fields such as automotive, aerospace and naval. Since design strategies require simple design parameters, the sound power is often used to characterize the sound radiated from a structure.

The CTSN in collaboration with TOP MODAL has recently developed a software tool to efficiently compute the radiated sound power of a vibrating structure using modes obtained by finite element analysis. The modal analysis has been enhanced to take into account the presence of fluid cavities and damping elements via the introduction of residual modes.

The radiated sound power is computed from the volume velocities of the vibrating surface using a lumped parameter method requiring no explicit modeling of the acoustic medium. The modal contributions to the total sound power may also be calculated.

The underlying methods are described including the improved coupled fluid-structure modal analysis and the computation of the radiated sound power. Next an overview of the tool's architecture is presented. Finally, an industrial application is presented to illustrate the features and interest of the tool.

## 1 Introduction

Often when studying the sound radiated from vibrating structures, a simple quantity characterizing the overall acoustic noise level is more useful than an abundance of data resulting from a detailed analysis. This is especially true in the design phase where efficient methods based on simple performance criteria are needed.

It is within this context that an innovative set of methods has been implemented within a software tool to compute the radiated sound power from the harmonic (steady-state) responses of vibrating structures.

The structure is modeled using finite elements with the radiating surface defined as a subset of the mesh - typically represented by plate elements and their associated nodes.

The finite element model can include acoustic cavities either totally enclosed by the structure or with openings to the external acoustic medium which can be included in the radiating surface.

Frequency responses calculations of a structure coupled with acoustic cavities are in general computationally intensive due to the unsymmetrical form of the coupled equations of motion which are often solved directly at each frequency step. To reduce the computational effort, the system can be reduced in size via a modal transformation using the *uncoupled* normal modes of the structure and acoustic cavities. Unfortunately the resulting condensed system may suffer in accuracy due to modal truncation errors - especially when dealing with heavy fluids such as water or highly pressurized gases. To overcome this problem, residual modes [1] have been appended to the normal modes of both the structure and fluid cavities to compensate for truncation effects.

Using the coupled equations of the condensed model, the frequency responses at the nodes of the radiating surface may be efficiently computed either directly or by mode superposition using the normal modes of condensed system. The mode superposition approach provides useful information about the contribution of each mode to the total response but may not be suitable for structures with strong localized damping in which case the responses should be computed directly.

A lumped parameter approach developed by Koopmann and Fahline [2] is used to compute the far-field sound power produced by the vibrating surface of the structure. No explicit modeling of the surrounding acoustic medium is required. Instead, a special form of the Kirchhoff-

Helmholtz equation is solved whose boundary conditions, expressed in terms of the volume velocities of the surface elements, are satisfied in an *average* or lumped parameter sense. This provides a good estimation of the far field pressure and corresponding radiated power where the averaging effects are negligible.

The first part of this paper presents the modal approach used to compute the frequency responses from the finite element model of a structure coupled with acoustic cavities. Next the lumped parameter method used to calculate the radiated sound power from the frequency responses is described. Finally, the software tool and an industrial application are presented.

## 2 Notations

### Scalars or matrices

$A, a$	coupling matrix, surface element length
$C, c$	damping, speed of sound
$F$	force
$i$	$\sqrt{-1}$
$K$	stiffness
$k$	mode, acoustic wave number ( $k = \omega / c$ )
$L$	characteristic length of structure
$M, m$	mass
$n$	unit vector
$p$	pressure
$Q$	acoustic cavity source
$S, s$	surface, acoustic source
$u, \hat{u}$	displacement, volume velocity
$v, \hat{v}$	velocity, normal velocity
$x$	position coordinates
$\eta$	hysteretic (structural) damping
$\Pi$	sound power
$\rho$	mass density
$\omega$	circular frequency $\omega = 2\pi f$
$\zeta$	modal viscous damping factor

### Subscripts

$b$	uncoupled structure and fluid mode ( $b=n+m$ )
$e$	surface element
$f$	fluid DOF
$k$	coupled mode
$s$	structure DOF
$n$	structure mode
$m$	fluid mode

### 3 Structural Responses

#### 3.1 Coupled Equations of Motion

The equations of motion governing the harmonic response of an structure comprising  $s$  degrees of freedom (DOF) coupled with one or more fluid cavities comprising  $f$  DOF are expressed below.

$$\left( -\omega^2 \begin{bmatrix} \mathbf{M}_{ss} & \mathbf{0}_{sf} \\ -\mathbf{A}_{fs} & \mathbf{M}_{ff} \end{bmatrix} + i\omega \begin{bmatrix} \mathbf{C}_{ss} & \mathbf{0}_{sf} \\ \mathbf{0}_{fs} & \mathbf{C}_{ff} \end{bmatrix} + \begin{bmatrix} \mathbf{K}_{ss} & \mathbf{A}_{sf} \\ \mathbf{0}_{fs} & \mathbf{K}_{ff} \end{bmatrix} \right) \begin{bmatrix} \mathbf{u}_s \\ \mathbf{p}_f \end{bmatrix} = \begin{bmatrix} \mathbf{F}_s \\ \dot{\mathbf{Q}}_f \end{bmatrix} \quad (1)$$

with :

- $\mathbf{M}_{ss}$  Structure mass matrix (symmetric)
- $\mathbf{C}_{ss}$  Structure viscous damping matrix (symmetric)
- $\mathbf{K}_{ss}$  Structure stiffness matrix (symmetric)
- $\mathbf{M}_{ff}$  Fluid "mass" matrix (symmetric)
- $\mathbf{C}_{ff}$  Fluid viscous damping matrix (symmetric)
- $\mathbf{K}_{ff}$  Fluid "stiffness" matrix (symmetric)
- $\mathbf{A}_{fs}$  Coupling matrix ( $\mathbf{A}_{sf} = \mathbf{A}_{fs}^T$ )
- $\mathbf{u}_s$  Vector of structural displacements
- $\mathbf{p}_f$  Vector of fluid pressures
- $\mathbf{F}_s$  Vector of forces applied to the structure
- $\mathbf{Q}_f$  Vector of acoustic sources ( $\dot{\mathbf{Q}}_f = i\omega\mathbf{Q}_f$ )

Damping may be introduced in the fluid cavities using acoustic absorbers (matrix  $\mathbf{C}_{ff}$ ), or as via hysteretic damping,  $\eta_f$ , which may be added to the stiffness matrix using  $(1+i\eta_f)\mathbf{K}_{ff}$ . Similarly, the structure may include both viscous and structural (hysteretic) damping.

Eq. (1) may be solved directly at each frequency,  $\omega$ , however the computation time may be overly prohibitive for large models ( $10^5$  or more DOF).

As an alternative, the modal reduction technique described hereafter has been developed to substantially reduce the computational effort.

#### 3.2 Uncoupled Normal Modes

The first step of the reduction process consists of computing the uncoupled normal modes of the structure and acoustic cavities as defined by the eigenvalue problems shown below.

$$(-\omega_n^2 \mathbf{M}_{ss} + \mathbf{K}_{ss}) \Phi_{sn} = \mathbf{0}_s \quad (2a)$$

$$(-\omega_m^2 \mathbf{M}_{ff} + \mathbf{K}_{ff}) \Phi_{fm} = \mathbf{0}_f \quad (2b)$$

This computation is relatively fast since each system is real and symmetric and may therefore be solved efficiently using for example the Lanczos method. The number of modes ( $n$  structural modes and  $m$  fluid modes) must include all modes up to the highest excitation frequency.

#### 3.3 Residual Modes

To minimize truncation errors, the structure and fluid normal modes  $\Phi_{sn}$  and  $\Phi_{fm}$  must be enriched by a set of residual modes that provide information about the coupling effects across the structure-fluid cavity boundaries.

A residual mode is similar to a normal mode in that it satisfies the same orthogonality properties and has an associated eigenvalue. However it does not satisfy the eigenvalue problem since each residual is in fact a particular linear combination of *all* the truncated (superior) normal modes.

Although residual modes (sometimes known as residual vectors or pseudo-modes) have been in use for well over a decade, their application to coupled analysis is recent [1] and has been implemented in this study. The procedure for deriving the residual modes is as follows.

For the structure, a set of  $m$  static modes  $\mathbf{X}_{sm}$  is computed resulting from the forces exerted by the fluid modes across the fluid-structure boundary.

$$\mathbf{K}_{ss} \mathbf{X}_{sm} = \mathbf{C}_{sf} \Phi_{sm} \quad (3)$$

Similarly for the fluid, a set of  $n$  static modes  $\mathbf{X}_{fn}$  is obtained using the pressure exerted by the structure modes across the same boundary but in the opposite sense.

$$\mathbf{K}_{ff} \mathbf{X}_{fn} = \mathbf{C}_{fs} \Phi_{fn} \quad (4)$$

Next, the static modes  $\mathbf{X}_{sm}$  and  $\mathbf{X}_{fn}$  are "filtered" or rendered orthogonal with respect to the normal modes  $\Phi_{sn}$  and  $\Phi_{fm}$ , and then orthogonalized to form an orthonormal basis of residual modes  $\hat{\Phi}_{sm}$  and  $\hat{\Phi}_{fn}$  which are then appended to the normal modes to form the enriched modal bases  $\mathbf{B}_{sn}$  and  $\mathbf{B}_{fm}$ . The subscripts  $n$  and  $m$  are conserved for the sake of simplicity.

$$\mathbf{B}_{sn} = [\Phi_{sn} \quad \hat{\Phi}_{sm}] \quad (5a)$$

$$\mathbf{B}_{fm} = [\Phi_{fm} \quad \hat{\Phi}_{fn}] \quad (5b)$$

#### 3.4 Condensed System and Responses

The physical system of Eq. (1) is condensed by replacing the physical responses  $\mathbf{u}_s$  and  $\mathbf{u}_f$  by the generalized responses  $\mathbf{u}_n$  and  $\mathbf{u}_m$  via the transformation of Eq. (6) to obtain the generalized equations of motion given in Eq. (7).

$$\mathbf{u}_s = \mathbf{B}_{sn} \mathbf{u}_n \quad \text{and} \quad \mathbf{u}_f = \mathbf{B}_{fm} \mathbf{u}_m \quad (6)$$

$$\left( -\omega^2 \begin{bmatrix} \mathbf{M}_{nn} & \mathbf{0}_{nm} \\ -\mathbf{A}_{mn} & \mathbf{M}_{mm} \end{bmatrix} + i\omega \begin{bmatrix} \mathbf{C}_{nn} & \mathbf{0}_{nm} \\ \mathbf{0}_{mn} & \mathbf{C}_{mm} \end{bmatrix} + \begin{bmatrix} \mathbf{K}_{nn} & \mathbf{A}_{nm} \\ \mathbf{0}_{mn} & \mathbf{K}_{mm} \end{bmatrix} \right) \begin{bmatrix} \mathbf{u}_n \\ \mathbf{p}_m \end{bmatrix} = \begin{bmatrix} \mathbf{F}_n \\ \dot{\mathbf{Q}}_m \end{bmatrix} \quad (7)$$

with :

$$\mathbf{F}_n = \mathbf{B}_{ns} \mathbf{F}_s, \quad \mathbf{p}_m = \mathbf{B}_{mf} \mathbf{p}_f, \quad \mathbf{M}_{nn} = \mathbf{B}_{ns} \mathbf{M}_{ss} \mathbf{B}_{sn}, \quad \text{etc.}$$

The condensed system of Eq. (7) may be solved either directly or by mode superposition using the  $k$  normal modes (including right *and* left eigenvectors  $\Phi_{bk}$  and  $Y_{bk}$ ) derived from the conservative condensed system with combined structure and fluid partitions ( $b = n + m$ ).

$$(-\omega_k^2 \mathbf{M}_{bb} + \mathbf{K}_{bb}) \Phi_{bk} = \mathbf{0}_{bk} \quad (8a)$$

$$\mathbf{Y}_{kb} (-\omega_k^2 \mathbf{M}_{bb} + \mathbf{K}_{bb}) = \mathbf{0}_{kb} \quad (8b)$$

$$\text{with } \mathbf{M}_{bb} = \begin{bmatrix} \mathbf{M}_{nn} & \mathbf{0}_{nm} \\ -\mathbf{A}_{mn} & \mathbf{M}_{mm} \end{bmatrix} \quad \mathbf{K}_{bb} = \begin{bmatrix} \mathbf{K}_{nn} & \mathbf{A}_{nm} \\ \mathbf{0}_{mn} & \mathbf{K}_{mm} \end{bmatrix}$$

The generalized masses are obtained from the orthogonality relation involving both right and left eigenvectors.

$$\mathbf{m}_k = \mathbf{Y}_{kb} \mathbf{M}_{bb} \Phi_{bk} \quad (9)$$

Due to the particular form of the system's asymmetry, it can be shown that the components of the right and left eigenvectors respect the following relation.

$$\begin{bmatrix} \mathbf{Y}_{nk} \\ \mathbf{Y}_{mk} \end{bmatrix} = \begin{bmatrix} \Phi_{nk} \\ \Phi_{mk} / \omega_k^2 \end{bmatrix} \quad (10)$$

Modal damping factors may be obtained from the diagonal terms of the generalized damping matrix according to

$$2\zeta_k = c_k / (m_k \omega_k) \quad (11)$$

$$\text{with } \mathbf{c}_k = \text{diag}(\mathbf{Y}_{kb} \mathbf{C}_{bb} \Phi_{bk}) \quad \text{and } \mathbf{C}_{bb} = \begin{bmatrix} \mathbf{C}_{nn} & \mathbf{0}_{nm} \\ \mathbf{0}_{mn} & \mathbf{C}_{mm} \end{bmatrix}$$

A similar procedure may be used to derive modal damping factors from the hysteretic (structural) damping in the stiffness matrices.

Note that use of modal damping assumes that the coupling (off-diagonal) terms in the generalized damping matrix are small. This assumption may not be valid for systems with strong localized damping, in which case Eq. (7) should be solved directly.

However if modal damping is applicable, then the responses may be efficiently calculated using mode superposition. For example, in the case of a force excitation applied to the structure, the displacement response in the structure is given by Eq. (12). The other response/excitation pairs may be obtained in a similar fashion.

$$\mathbf{u}_s(\omega) = \sum_k \frac{1}{m_k} \left[ \frac{\mathbf{B}_{sn} \Phi_{nk} \Phi_{kn} \mathbf{B}_{ns}}{\omega_k^2 - \omega^2 + i 2\zeta_k \omega_k \omega} \right] \mathbf{F}_s(\omega) \quad (12)$$

Finally the nodal velocities within the structure are given by  $\mathbf{v}_s = i\omega \mathbf{u}_s$  from which the volume velocities of the radiating surface may be derived for the computation of the radiated sound power.

If the fluid cavities are in contact with the external acoustic medium, it may be desirable to include the opening of the fluid cavity as part of the radiating surface. To do so, the normal component of the fluid velocity at the cavity opening may be computed from the gradient of the pressure using Euler's equation.

$$\mathbf{v}(\mathbf{x}) \cdot \mathbf{n} = \frac{1}{i\omega\rho} \nabla \mathbf{p}(\mathbf{x}) \cdot \mathbf{n} \quad (13)$$

These fluid velocities may then be included among the structure velocities of the radiating surface.

## 4 Radiated Sound Power

### 4.1 Introduction

Consider the radiating surface of the structure depicted in Fig. 1 with characteristic length,  $L$ , and composed of surface elements,  $e$ , with characteristic length  $a$  related to the mesh size of the finite element model.

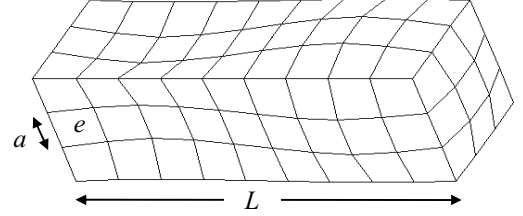


Fig. 1 : Radiating Surface and Elements

The normal velocities at the element's nodes,  $\hat{v}_n$ , may be decomposed into an average or piston-like component,  $\hat{v}_e$ , and a zero-average component as depicted in Fig. 2 using a one-dimensional element for the sake of simplicity.

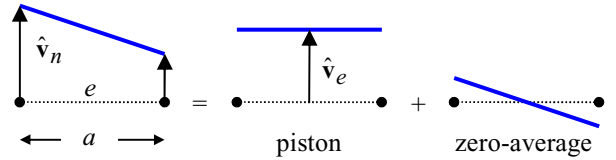


Fig. 2 : Element Normal Velocities

Another important parameter is the acoustic wavenumber,  $k = \omega/c$ , whose inverse,  $1/k$  is the acoustic wavelength.

If each element of the radiating surface is small compared to the acoustic wavelength, ( $ka \ll 1$ ), then the far field acoustic radiation can be well approximated using the piston motion only and its associated volume velocity  $\hat{u}_e = \hat{v}_e \cdot S_e$  with  $S_e$  the surface area of the element.

In particular we are interested in estimating the far field power output - a simple quantity useful in characterizing the overall radiated noise as a function of frequency.

At very low frequencies ( $kL \ll 1$ ), the sound power,  $\Pi$ , can be approximated using a simple acoustic source whose volume velocity is equal to the overall volume velocity of the radiating surface as defined below.

$$\Pi_{LF} = \frac{k^2 \rho c}{8\pi} \left| \sum_e \hat{u}_e \right|^2 \quad (14)$$

At very high frequencies ( $kL \gg 1$ ), the power output can be computed using a plane wave approximation applied to each element as follows.

$$\Pi_{HF} = \frac{\rho c}{2} \sum_e |\hat{v}_e|^2 S_e \quad (15)$$

These approximations are useful, but often in practice the frequency ranges of interest are those where the acoustic wavelength is of the same order as the radiating surface ( $kL \approx 1$ ), in which case a numerical solution is required as described hereafter.

## 4.2 Sound Power Computation

A lumped parameter approach based on a volume velocity matching scheme developed by Koopmann [2] is used to compute the far field sound power. Starting from the Kirchhoff-Helmholtz integral equation, the following approximate solution for the acoustic pressure field may be derived expressed in terms of the free-space Green's function  $\hat{\mathbf{g}}$  and constant coefficients  $\alpha_V$  and  $\beta_V$ .

$$\hat{\mathbf{p}}(\mathbf{x}) = \sum_{\nu=1}^N \hat{\mathbf{s}}_{\nu} \left\{ \alpha_{\nu} \hat{\mathbf{g}}(\mathbf{x}, \mathbf{x}_{\nu}) + \beta_{\nu} [\nabla \hat{\mathbf{g}}(\mathbf{x}, \mathbf{x}_{\nu}) \cdot \mathbf{n}_s]_{\mathbf{x}_s = \mathbf{x}_{\nu}} \right\} \quad (16)$$

In Eq. (16) an acoustic source of amplitude,  $\hat{\mathbf{s}}_{\nu}$ , is assumed to be located at the geometrical center of each surface element and of type monopole ( $\alpha_{\nu}=1, \beta_{\nu}=0$ ), dipole ( $\alpha_{\nu}=0, \beta_{\nu}=i/k$ ) or tripole ( $\alpha_{\nu}=1, \beta_{\nu}=i/k$ ). A monopole is used for baffled elements, a dipole for elements enclosing no volume, and a tripole for elements enclosing a finite volume.

Eq. (16) can be rewritten in terms of the velocity using Euler's equation, and then integrated over the element surface to obtain a system of equations relating the volume velocities,  $\hat{\mathbf{u}}$ , to the sources,  $\hat{\mathbf{s}}$  at the element centers.

$$\hat{\mathbf{u}} = \mathbf{U} \hat{\mathbf{s}} \quad (17)$$

The terms of  $\mathbf{U}$  are computed using the following integral.

$$U_{\mu\nu} = \frac{1}{ik\rho c} \iint_{S_{\mu}} \nabla \left\{ \alpha_{\nu} \hat{\mathbf{g}}(\mathbf{x}, \mathbf{x}_{\nu}) + \beta_{\nu} [\nabla \hat{\mathbf{g}}(\mathbf{x}, \mathbf{x}_{\nu}) \cdot \mathbf{n}_s]_{\mathbf{x}_s = \mathbf{x}_{\nu}} \right\} \mathbf{n} dS(\mathbf{x}) \quad (18)$$

Once the source amplitudes are determined from Eq. (17), they are used to compute the acoustic power output based on analytic expressions for the power output of simple, dipole and tripole sources. This computation is expressed in matrix form below. Details on the mathematical formulation of the matrix  $\mathbf{S}$  can be found in [2].

$$\mathbf{\Pi} = \hat{\mathbf{s}}^H \mathbf{S} \hat{\mathbf{s}} \quad (19)$$

## 4.3 Modal Contributions

If the surface responses are calculated using mode superposition, then modal volume velocities may be defined using

$$\hat{\mathbf{u}}_{ek} = i\omega_k \mathbf{T}_{es} \mathbf{B}_{sn} \mathbf{\Phi}_{nk} \quad (20)$$

with  $\mathbf{B}_{sn} \mathbf{\Phi}_{nk}$  from Eq. (12) and  $\mathbf{T}_{es}$  representing the geometrical transformation from the nodal displacements to the average surface element displacement. The modal volume velocities can be helpful in describing and understanding the behavior of the radiating surface.

The physical volume velocities may then be expressed using mode superposition by substituting Eq. (20) into Eq. (12) as shown below.

$$\hat{\mathbf{u}}(\omega) = \sum_k \frac{1}{m_k} \left[ \frac{\hat{\mathbf{u}}_{ek} \mathbf{\Phi}_{kn} \mathbf{B}_{ns}}{\omega_k^2 - \omega^2 + i2\zeta_k \omega_k \omega} \right] \mathbf{F}_s(\omega) \quad (21)$$

Using Eq. (21), it is also possible to compute the power output of each mode,  $k$ , at the frequency  $\omega = \omega_k$  in order to assess the contribution of each mode to the total power output at the resonant peaks.

## 5 Implementation

### 5.1 Software Description

In order to perform and manage the various calculations described above, the software tool VIAC written in MATLAB has been developed (see Fig. 3). The tool is interfaced with the finite element code MSC/NASTRAN and with POWER, a FORTRAN code for the sound power computation developed by Koopmann and Fahline [2].

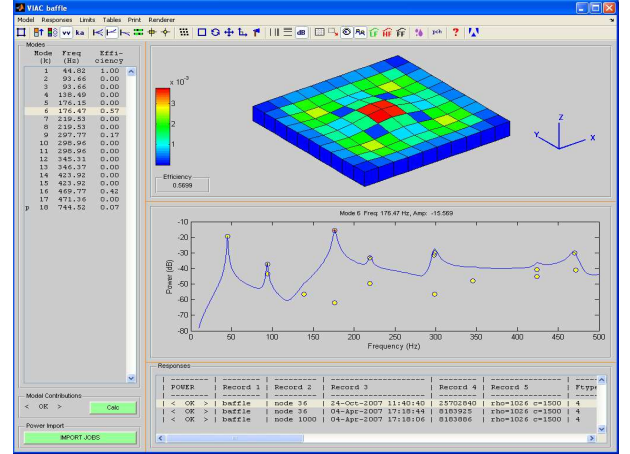


Fig. 3 : VIAC User Interface

The frequency responses at the vibrating surface of the structure are first computed using NASTRAN. In the presence of fluid cavities, a special DMAP (Direct Matrix Abstraction Program) script is included to generate the residual modes described in §3.3. The responses are then calculated from the condensed coupled system of Eq. (7) either directly or via mode superposition for lightly or uniformly damped structures.

The responses are then imported to VIAC where they are converted to volume velocities and plotted on the mesh of the radiating surface. The low and high frequency approximations of Eq. (14-15) may also be calculated using the volume velocities.

The sound power is computed using the POWER routine which requires as input the geometry of the surface elements, the source types (simple, dipole or tripole), and the volume velocities as a function of frequency. To reduce the computation time, the sound power calculation may be distributed over several machines and/or CPUs by dividing the volume velocities into separate frequency bands and then recombining the power output responses in VIAC.

If mode superposition is used to compute the surface responses, the modal volume velocities and modal contributions to the power output may be calculated and plotted in VIAC. Several functions are available to verify the orientation and other properties of the radiating surface as shown below.

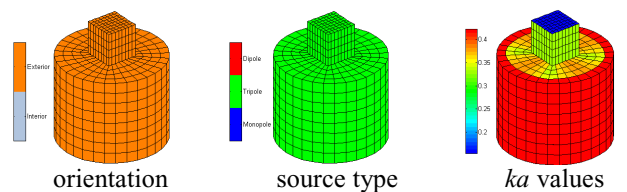


Fig. 4 : Properties of the Radiating Surface

## 5.2 Industrial Application

A study was carried out using the VIAC software tool in order to study the behavior of a ventilation duct of a marine structure.

The finite element model of the ventilation duct is shown at left in Fig. 5. Air enters the circuit at the top right inlet port and then splits into the two exhaust ducts before exiting into the compartment shown at right with the duct on the inner wall.

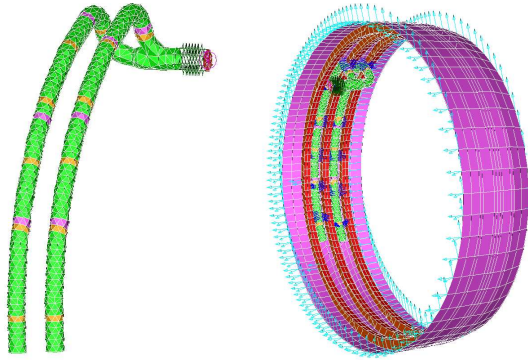


Fig. 5 : FE Model of Duct and Compartment

The air on the inside of both the compartment and ducts is modeled using two fluid cavities (not shown) with a coincident interface at the two exhaust outlets. A layer of acoustic absorber elements is added to the two faces of the compartment fluid cavity to minimize unwanted wave reflection.

The radiating surface under consideration is that of the duct including the two outlet ports. Since the outlet ports have no associated surface elements, normal velocities were computed using the pressure field gradient according to Eq. (13) in order to include the two outlet ports in the radiating surface.

Following a modal analysis of the coupled system based on Eq. (8), the modal strain and kinetic energies were computed in order to identify the dominant structure and fluid modes according to the energy distribution. In Fig. 6 we see limited coupling in the energies and therefore the fluid modes (shown in boldface) and structure modes are easy to identify.

Mode (k)	Kinetic			Strain		
	M <sub>ss</sub>	M <sub>ff</sub>	M <sub>tot</sub>	K <sub>ss</sub>	K <sub>ff</sub>	K <sub>tot</sub>
1						
2	0.98	0.11	1.09	0.89	0.02	0.91
3	0.99	0.00	0.99	1.00	0.01	1.01
4	0.93	0.04	0.98	0.96	0.07	1.02
5	0.99	0.00	0.99	1.00	0.01	1.01
6	<b>0.17</b>	<b>0.85</b>	<b>1.02</b>	<b>0.15</b>	<b>0.83</b>	<b>0.98</b>
7	0.91	0.10	1.01	0.90	0.09	0.99
8	0.99	0.00	1.00	1.00	0.01	1.00
9	0.99	0.00	0.99	1.00	0.01	1.01
10	0.99	0.00	0.99	1.00	0.01	1.01
11	0.99	0.00	0.99	1.00	0.01	1.01
12	<b>0.00</b>	<b>1.00</b>	<b>1.00</b>	<b>0.00</b>	<b>1.00</b>	<b>1.00</b>
13	<b>0.09</b>	<b>0.91</b>	<b>1.00</b>	<b>0.09</b>	<b>0.91</b>	<b>1.00</b>
14	0.91	0.09	1.00	0.91	0.09	1.00
15	0.94	0.06	1.00	0.94	0.06	1.00
16	<b>0.06</b>	<b>0.94</b>	<b>1.00</b>	<b>0.06</b>	<b>0.94</b>	<b>1.00</b>
17	0.99	0.00	0.99	1.00	0.01	1.01
18	<b>0.00</b>	<b>1.00</b>	<b>1.00</b>	<b>0.00</b>	<b>1.00</b>	<b>1.00</b>
19	0.99	0.00	0.99	1.00	0.01	1.01
20	<b>0.00</b>	<b>1.00</b>	<b>1.00</b>	<b>0.00</b>	<b>1.00</b>	<b>1.00</b>

Fig. 6 : Modal Energy Distribution (normalized)

The system was excited by applying a pressure at the inlet port via a massless rigid piston coupled to the fluid cavity.

The sound power was calculated with and without the exhaust ports in order to determine their contribution to the output power. The sound power responses plotted in Fig. 7 show that the majority of the radiated power comes from the two exhaust ports and that the radiation from the ducts' surface is negligible over the entire frequency range.

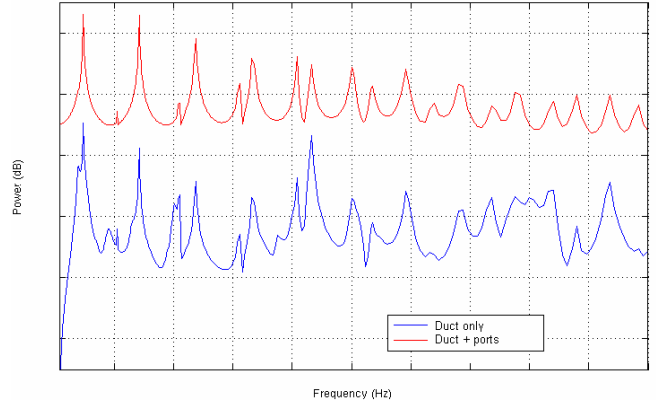


Fig. 7 : Influence of Output Ports on Sound Power

Sound power responses were also compared between two ventilation ducts with different geometries to see if significant differences in measured power levels between the two systems in a critical frequency range could be accounted for analytically. The results are plotted in Fig. 8 and appear to corroborate the experimental measurements.

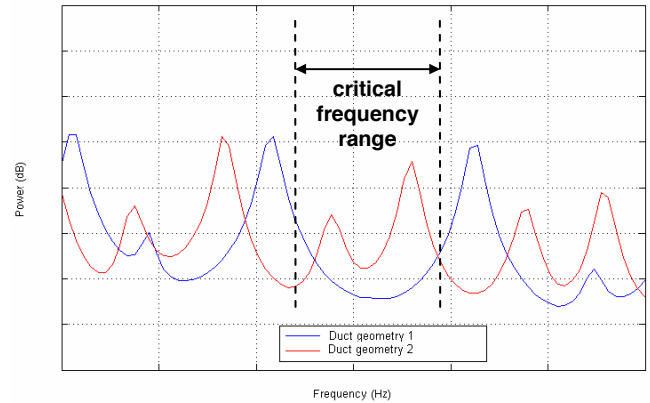


Fig. 8 : Sound Power from Different Duct Geometries

## Acknowledgments

This work was funded primarily by the DGA/CTSN under the contract N° 05 61 554 00.

## References

- [1] N. Roy, A. Girard, *Impact of residual modes in structural dynamics*, Proceedings, European Conference on Spacecraft Structures, Materials and Mechanical Testing, Noordwijk, The Netherlands, May 2005.
- [2] G. H. Koopmann, J. B. Fahnlne, *Designing Quiet Structures - A Sound Power Minimization Approach*, Academic Press, 1997.